Substituent Effects on Dynamics at Conical Intersections: Cyclopentadienes

Oliver Schalk, Andrey E. Boguslavskiy, and Albert Stolow*

Steacie Institute for Molecular Sciences, National Research Council, Ottawa, Ontario K1A 0R6, Canada

Received: November 27, 2009; Revised Manuscript Received: January 29, 2010

Substituent effects on dynamics at conical intersections are investigated by means of femtosecond time-resolved photoelectron spectroscopy for cyclopentadiene and its substituted analogues 1,2,3,4-tetramethylcyclopentadiene, 1,2,3,4,5-pentamethylcyclopentadiene, and 1,2,3,4-tetramethyl-5-propylcyclopentadiene. By UV excitation to the S_2 (1^1B_2) state, the influence of these substitutions on dynamics for the initially excited S_2 (1^1B_2) surface and the spectroscopically dark S_1 (2^1A_1) surface were investigated. We observed that the dynamics depend only on a small number of specific vibrations. Whereas dynamics at the S_2/S_1-conical intersection are independent of substitution at the 5-position, internal conversion dynamics on the S_1 (2^1A_1) surface slow down as the inertia of the 5-substituent increases. Contrary to the expectations of simple models of radiationless transitions, an increasing density of states does not lead to faster processes, suggesting that a true dynamical picture of vibrational motions at conical intersections will be required.

1. Introduction

The description of excited state nonadiabatic dynamics in polyatomic molecules increasingly recognizes the importance of conical intersections (CI's).[1−3] This is so because CI's play a role in excited state dynamics analogous to that of the "transition state" in ground state dynamics. For ground state reaction dynamics, the "Polanyi rules"[4] lucidly relate the topographical features of the "transition state", the inertia of the reacting atoms and the energetics, to the outcomes and energy disposal of the reaction. For example, ground state A + BC reactions with "late" transition state barriers are more favorably traversed by vibrationally excited BC reactants, as opposed to "early" barriers that are more favorably crossed by high velocity collisions. Unfortunately, an analogous set of Polanyi rules for excited state polyatomic dynamics does not yet exist. Efforts to systematize the topography (e.g., tilt and asymmetry) of CI's has begun. In particular, Atchity et al.[5] and Yarkony[3] classified CI's into "peaked" and "sloped" categories. Peaked topographies, i.e., when the CI is located at a local minimum of the upper potential energy surface, are expected to lead to fast internal conversion by funneling trajectories toward the CI. In contrast, sloped topographies, when the CI is located away from a potential minimum, can lead to trajectories recrossing the CI, slowing the internal conversion rate. By analogy with the Polanyi rules, we might expect that specific vibrational dynamics at the CI will be as important to the dynamics as are the topographical features of the CI. Furthermore, we expect that specific molecular motions (both in their amplitude and in speed) will promote or hinder nonadiabatic crossings of the excited state trajectory: as in the well-known 1D Landau−Zener avoided crossing problem,[6,7] the (multidimensional) velocity of the trajectory near a CI should affect the adiabatic vs diabatic branching ratio. Dynamics at CI's will be dependent on a number of factors. The first, trivial concern is whether or not the CI is energetically accessible from the initially excited state. This in and of itself, however, is insufficient in determining the importance of that CI to the overall dynamics. For example, the CI may be conformationally inaccessible or have topological features that render it impotent. There exists a need to develop fully dynamical theories of processes at conical intersections from which, we hope, "rules of thumb" (multidimensional analogues of the Polanyi rules) may be distilled. We believe phenomenological investigations, such as the effects of substituents, are useful at this stage. Systematic chemical substitutions were used to discern the roles of electronic structure, density of states, and floppiness or rigidity in electronically nonadiabatic dynamics in substituted benzenes[8] and ethylenes.[9] Further studies on a substituted ethylene directly revealed vibrational wavepacket motions induced by passage through a conical intersection.[10] In a recent, detailed study on excited state dynamics in the α,β-enones,[11] the location of a methyl substituent on acrolein (2-propenal) was shown to lead to very different photodynamics, despite the relative energetics and topologies of the CI's being very similar for all molecules concerned. This provided a clear example of the dynamical importance of specific vibrational motions at conical intersections.

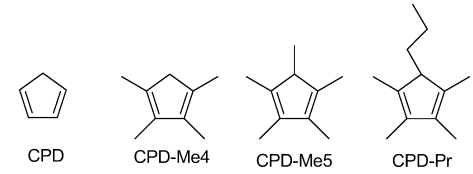

Figure 1. Molecular structures of cyclopentadiene (CPD), 1,2,3,4-tetramethylcyclopentadiene (CPD-Me4), 1,2,3,4,5-pentamethylcyclopentadiene (CPD-Me5) and 1,2,3,4-tetramethyl-5-propylcyclopentadiene (CPD-Pr).

Here we use methyl substitution to study the excited state dynamics of a prototypical polyatomic molecule, cyclopentadiene (CPD). Its methylated derivatives employed here are 1,2,3,4-tetramethylcyclopentadiene (CPD-Me4), 1,2,3,4,5-pentamethylcyclopentadiene (CPD-Me5), and 1,2,3,4-tetramethyl-5-propylcyclopentadiene (CPD-Pr); see Figure 1 for molecular structures. We used the technique of time-resolved photoelectron spectroscopy (TRPES)[12−14] to study the excited state dynamics. This scheme is depicted in Figure 2. Compared with acrolein,[11] CPD has higher symmetry (C_{2v}) but exhibits symmetry breaking in the 5-substituted molecules, permitting a simplified analysis.

* Corresponding author. E-mail: albert.stolow@nrc.ca.

10.1021/jp911286s Published 2010 by the American Chemical Society
Published on Web 03/01/2010

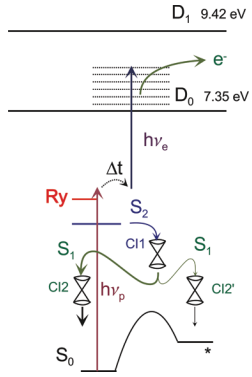

Figure 2. Proposed scheme for excited state dynamics in cyclopentadienes. The pump pulse ($h\nu_p$) can excite either the S_2 (blue) or, in the case of $\lambda_p = 240$ nm, the lowest lying Rydberg state (Ry, red). The conical intersections between S_1 and S_2, labeled CI1, lead via population decay to the S_1 state. On the S_1 potential energy surface, we suggest that the dominant decay pathway is to S_0 via the conical intersection CI2. There may be another intersection CI2′ that decays to S_0 via a metastable BP intermediate (∗), although we have no direct proof of this. See section 4 for further details.

In addition, the rigidity of the ring structures favors a Franck−Condon analysis of the photoelectron spectra. Finally, the vibrational density of states increases systematically from CPD-Me4 to CPD-Pr, as opposed to the acrolein derivatives where it remained roughly constant.[11] For the case of CPD and its perdeuterated variant, a model for the UV-excited state dynamics was proposed by Fuss et al. on the basis of ultrafast intense-field dissociative ionization studies.[15] In this model, a UV photon excites the molecule from the ground state (S_0, 1^1A_1) to the S_2 state (1^1B_2). Within $\tau_1 \approx 40$ fs, the dynamics reaches the S_1 surface (2^1A_1) from where two reaction paths are possible. One returns the system to the ground state within 50 fs via an [1, 3]-H shift, as indicated by the perdeuterio experiments (see Figure 2 and section 4 for a more detailed discussion on this proposed mechanism). The other path may lead to either bicyclic or tricyclic products (bicyclo[2,1,0]pentene (BP) or tricyclo[2,1,0,0]pentane (TP)), as found in continuous irradiation experiments.[16−18]

We expect that methyl substitution will have only very minor effects on the topology of the relevant conical intersections, on the basis of previous experience with the methyl substituted enones.[11] In this situation, we can approximate the main effects of methyl substitution as (i) adding inertia to specific vibrational motions and (ii) changing the vibrational density of states. Is it the internal structure of the methyl groups or is it their inertia, equivalent to a hypothetical ^{15}H atom, which governs the dynamics? This question is related to the famous "ring + tail" problem[19−21] regarding the influence of internal vibrational redistribution (IVR) due to a molecular "tail", such as an alkyl chain, on the optical properties of a chromophore (ring). However, further analysis of the differences in the fluorescence spectra of monoalkylated benzenes could be explained by considering only the Franck−Condon spectrum, without including IVR.[21] This calls into question the role of the total density of vibrational states. In the present experiments, a possible dependence of the dynamics on the Franck−Condon spectrum was addressed by variation of the excitation wavelength.

In the following sections, our TRPES method is briefly described (section 2). The time-resolved photoelectron spectra of the various substituted and the unsubstituted cyclopentadienes are presented in section 3 and discussed in section 4. A short conclusion and outlook follow.

2. Experiment

CPD-Me4, CPD-Me5, and CPD-Pr were obtained from Sigma-Aldrich with nominal purities of 85%, 97%, and 98%, respectively, and used without further purification. CPD was prepared by cracking the dimer at 440 K and diluting it in a ratio of 1:100 in He. UV−vis spectra were recorded with a Varian 5e-spectrometer, evaporating the samples in a quartz cuvette at 50 °C. TRPES experiments were performed in a molecular beam, magnetic bottle photoelectron spectrometer that was previously described in detail.[22] Briefly, femtosecond laser pulses were obtained from a Ti:sapphire regenerative amplifier (Coherent, Legend), pumped by two 1 kHz Nd:YLF lasers (Positive Light, Evolution). The seed beam (800 nm) was provided by a Ti:sapphire oscillator (Spectra Physics, Tsunami) pumped by a Nd:YLF diode laser (Spectra Physics, Millennia). Pump laser pulses tunable between $\lambda_p = 240$ nm and $\lambda_p = 278$ nm were obtained by frequency doubling a femtosecond pulse generated by frequency mixing the output of an optical parametric amplifier (TOPAS, Light Conversion) with the fundamental pulse. The probe laser pulse at $\lambda_e = 322$ nm was obtained by fourth harmonic generation of the output of a second TOPAS. In experiments, the laser beams were attenuated to 500 nJ and 2 μJ for pump and probe pulse, respectively, and focused weakly into the interaction region by a concave spherical aluminum mirror (*f*/150 for the pump and *f*/125 for the probe pulse, ensuring a smaller spot size of the probe pulse in the interaction region). The polarization directions of the linearly polarized pulses were controlled by Berek compensators (New Focus) and were set to magic angle with respect to each other. The cross-correlation between pump and probe pulses was measured by the rise time of diazabicyclo[2,2,2]octane ionization and was determined to be $\tau_{cc} = 160$ fs, depending slightly on the wavelength of the pump pulse. The spectral bandwidth of each of the pump and the probe pulses was around 200 cm^{-1}. The time delay between the two pulses was controlled by a motorized linear translation stage. Perpendicular to the incoming laser pulses, a high intensity, skimmed pulsed supersonic molecular beam (1 kHz Even-Lavie valve, 250 μm diameter, concical nozzle) passed through the interaction region. The stagnation pressure of the He carrier gas was 3 bar. The organic sample was introduced by filter paper soaked with the liquid cyclopentadiene derivative. At each time delay, the measured pump−probe signal was corrected by dynamically subtracting the background signals due to the pump and probe laser pulses alone.

3. Results

3.1. UV Spectra. The UV-spectra of CPD (black), CPD-Me4 (black dashed), CPD-Me5 (gray), and CPD-Pr (gray dashed) are shown in Figure 3, normalized with respect to their first maximum. While the absorption spectrum of CPD only shows weak structures (spectra with higher resolution can be found in refs 23 and 24), the methylated derivatives exhibit broad and irregularly structured bands. The absorption maxima range systematically from 5.17 eV (240 nm) for CPD to 4.88 eV (254 nm) for CPD-Pr.

3.2. Time-Resolved Photoelectron Spectra. Pump−probe TRPES-studies of CPD-Me4, CPD-Me5, and CPD-Pr were performed at pump wavelengths of $\lambda_p = 240$, 250, 258, and 278 nm and probed at $\lambda_e = 322$ nm. The total photon energies of pump plus probe photon were thus 9.05, 8.84, 8.69, and 8.34 eV, respectively. In all cases, the pump photon energies were within the relevant absorption band of the molecules (see Figure 3). Typical TRPES spectra of CPD-Pr, at all four pump

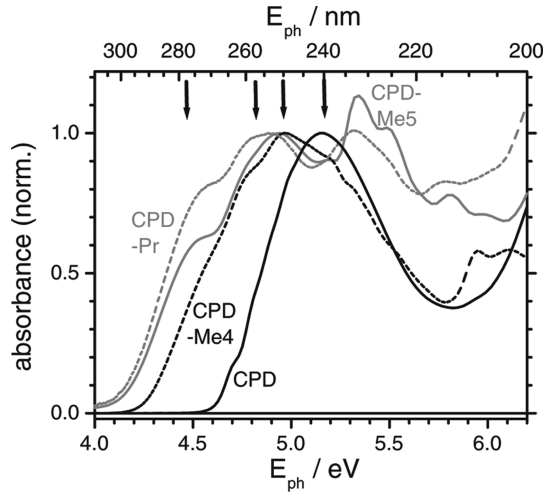

Figure 3. UV absorption spectra of cyclopentadiene (CPD, black), 1,2,3,4-tetramethylcyclopentadiene (CPD-Me4, black, dashed), 1,2,3,4,5-pentamethylcyclopentadiene (CPD-Me5, gray) and 1,2,3,4-tetramethyl-5-propylcyclopentadiene (CPD-Pr, gray, dashed). The arrows indicate the femtosecond pump laser excitation energies used in the TRPES experiments.

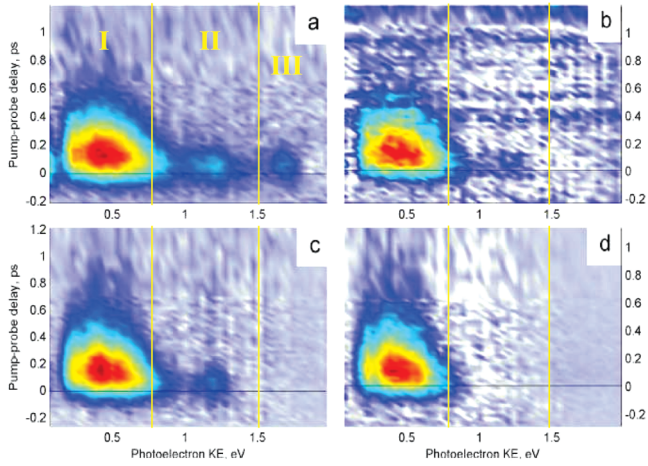

Figure 4. Time resolved photoelectron spectra of CPD-Pr at pump wavelengths of (a) 240 nm, (b) 250 nm, (c) 258 nm, and (d) 278 nm. The probe wavelength was $\lambda_e = 322$ nm in all cases.

wavelengths, are shown in Figure 4. The TRPES spectra of CPD-Me4 and CPD-Me5 are similar in form (not shown). In Figure 4a ($\lambda_p = 240$ nm), two bands appear around time zero. One lies around 1.7 eV electron kinetic energy (herein referred to as region III) and is rather sharp, while the other extends over a broad kinetic energy region between 0.75 and 1.5 eV, peaking around 1.2 eV (region II). Shifted toward positive time delays, a broad peak appears between 0.2 and 0.7 eV (region I). The spectra of CPD-Me4 and CPD-Me5 are red-shifted by ~0.1 and 0.05 eV, respectively, except for the peak in region III, which remains invariant. At $\lambda_p = 250$ nm and $\lambda_p = 258$ nm, the spectra appear similar but the band in region III is now absent. At $\lambda_p = 278$ nm, the band at 1.2 eV is now also missing, since the energy threshold for these spectra lies between 0.9 and 1 eV in a [1+1′] experiment (one photon pump, one photon probe experiment).

The TRPES spectra can be rationalized as follows. The ionization potentials to the ionic ground (D_0) and first excited state (D_1) of CPD-Me5 were observed at 7.35 and 9.42 eV, respectively, by means of He I photoelectron spectroscopy.[25] For CPD-Me4 and CPD-Pr, no photoelectron spectra were

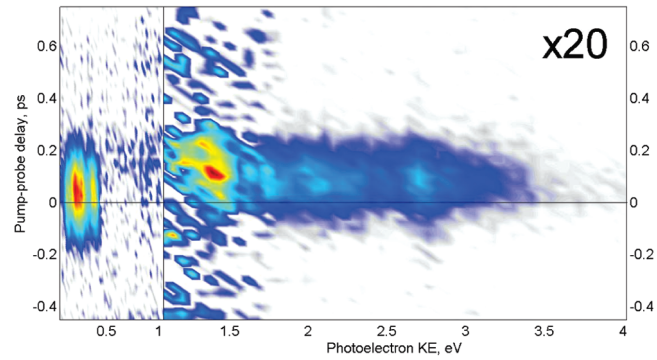

Figure 5. Time resolved photoelectron spectrum of CPD at a pump wavelength of $\lambda_p = 240$ nm and a probe wavelength of $\lambda_e = 322$ nm. The high energy region (photoelectron kinetic energy >1 eV is multiplied by a factor of 20. This region corresponds to two-photon ionization of the excited states.

reported but the similarities between our TRPES spectra indicate that the ionization energies should be quite similar. The total energy of pump plus probe photons is 9.05 eV ($\lambda_p = 240$ nm) and exceeds the ionization potential to D_0 by 1.7 eV. This is the maximal kinetic energy that can be transferred to photoelectrons and correlates with the energy cutoff found in our experimental data (Figure 4). Since the D_1 and higher excited ionic states cannot be energetically accessed, they are not considered further. The peak in region I is shifted in time and originates from dynamics on a lower lying state (S_1 state; see Figure 2). Since it appears at lower kinetic energy, some excess energy must be redistributed among vibrational modes during internal conversion of these states. At lower pump photon energy, no signal appears in region III, indicating that the lower excited state is not longer energetically accessible by single probe photon ionization. Regions I and II remain unchanged, due to invariant Franck−Condon overlap of the excited states with the ionic ground state. At $\lambda_p = 278$ nm, the maximal electron kinetic energy for a [1+1′] experiment is 0.99 eV and, therefore, the peak at 1.2 eV is no longer observed.

The TRPES spectrum of CPD at a pump wavelength of $\lambda_p = 240$ nm and a probe wavelength of $\lambda_e = 322$ nm is shown in Figure 5. Here a signal at $\Delta t = 0$ appears at low energies, between 0.1 and 0.45 eV. It is weakly structured with maxima at 0.4 and 0.2 eV. A broad, delayed and much weaker signal is found throughout the whole spectrum (although it might be hidden under the dominant signal in the low energy region of the spectrum). The ionization potentials to the ionic ground and the first ion excited state were observed at 8.57 eV and at 10.62 eV by He I photoelectron spectroscopy.[26,27] One probe photon suffices to ionize the initially excited S_2 state. However, two photons seem to be necessary for ionizing the lower lying S_1 state.

Time constants and their associated photoelectron spectra were determined by a standard Levenberg−Marquart global fitting routine wherein the 2D data $S(E,\Delta t)$ are expressed as

$$S(E,\Delta t) = \sum_i A_i(E) \cdot P_i(\Delta t) \otimes g(\Delta t) \qquad (1)$$

where $A_i(E)$ is the decay associated photoelectron spectrum of the ith channel, which has a time dependent population $P_i(\Delta t)$, and $g(\Delta t)$ is the experimentally determined Gaussian cross-correlation function. Although in some cases this representation of the data may be misleading, such as when there are large amplitude motions,[11] it is nevertheless a useful zeroth-order description of

TABLE 1: Global Fit Parameters for the Experiments on Cyclopentadiene Derivatives at Various Pump Wavelengths λ_p[a]

	$\lambda_p = 240$ nm		$\lambda_p = 250$ nm		$\lambda_p = 258$ nm		$\lambda_p = 278$ nm	
	τ_1	$\begin{pmatrix}\tau_2\\ \tau_2/\tau_3\end{pmatrix}$[b]	τ_1	$\begin{pmatrix}\tau_2\\ \tau_2/\tau_3\end{pmatrix}$	τ_1	$\begin{pmatrix}\tau_2\\ \tau_2/\tau_3\end{pmatrix}$	τ_1	$\begin{pmatrix}\tau_2\\ \tau_2/\tau_3\end{pmatrix}$
CPD	$\begin{pmatrix}39\\ 20 \pm 23^c\end{pmatrix}$	$\begin{pmatrix}51\\ 71/33^c\end{pmatrix}$						
CPD-d_6[c]	29 + 23	114/440						
CPD-Me4	71	74	68	76	66	$\begin{pmatrix}124\\ 84/680\end{pmatrix}$	77	$\begin{pmatrix}111\\ 94/380\end{pmatrix}$
CPD-Me5	71	$\begin{pmatrix}127\\ 111/700\end{pmatrix}$	79	$\begin{pmatrix}123\\ 112/700\end{pmatrix}$	72	$\begin{pmatrix}133\\ 102/700\end{pmatrix}$	50	$\begin{pmatrix}195\\ 112/710\end{pmatrix}$
CPD-Pr	69	168	72	179	77	174	78	186

[a] The probe wavelength was $\lambda_e = 322$ nm. Errors were usually around 15%. [b] Two time constants are given for the cases where the introduction of a third time constant nontrivially improved the fit. [c] Values from intense field dissociative ionization studies.[15] In these experiments, two time constants were found to describe the dynamics on the S_2 surface.

the dynamics. The merit of this representation is confirmed in the present case by investigating the time behavior of specific slices of the data at fixed photoelectron kinetic energies.

To begin, the 2D data were cut into 1D energy slices of width $\Delta E = 0.05$ eV. The time dependence of these slices were fitted by a convolution of the Gaussian cross-correlation function $g(\Delta t)$ with an exponential decay. The dynamics in regions II and III were modeled by a single exponential decay. These regions could be fitted with the same time constant $\tau_1 = 70 \pm 15$ fs for all methylated cyclopentadienes, irrespective of substitution in the 5-position or the pump wavelength. Subsequently, the 2D spectrum was fitted by fixing the first time constant τ_1. The extracted time constants are given in Table 1. In most cases, a second time constant (τ_2) was sufficient to accurately but nontrivially describe the TRPES spectra. For CPD-Me5 and CPD-Me4 at $\lambda_p = 258$ and 278 nm, a third time constant (τ_3) could nontrivially improve the reduced χ^2 of the fit. The second time constant (τ_2) depended systematically on substitution in the 5-position but showed little dependence on the pump wavelength. For CPD-Me4, we found a time constant of $\tau_2 = 70 \pm 10$ fs, for CPD-Me5 $\tau_2 = 110 \pm 15$ fs, and for CPD-Pr $\tau_2 = 175 \pm 20$ fs.

As an example, the decay associated photoelectron spectra $A_{\tau_i}(E)$ for $\lambda_p = 240$ nm for CPD-Pr are shown in Figure 6. In the $A_i(E)$, positive amplitudes represent an exponential decay of the signal whereas a negative amplitude is associated with an exponential rise. In the region of high photoelectron kinetic energy $E > 0.75$ eV, only single exponential decay of the initially populated state(s) is seen, hence $A_{\tau_1} \neq 0$ and $A_{\tau_2} = 0$. As discussed in section 4.3, this part can be further divided into two bands that are populated upon photoexcitation: the S_2 band in region II, and a Rydberg band (Ry) in region III. In region I, the population dynamics of the lower lying S_1 state is seen in $A_{\tau_2}(E)$ and ultimately $A_{\tau_3}(E)$. The rise time for the S_1 population, which grows at a rate given by τ_1, manifests itself as a negative amplitude A_{τ_1}. In Figure 7 we show decay-associated photoelectron spectra $A_{\tau_i}(E)$ for $\lambda_p = 240$, 258, and 278 nm. Here, the similarities between the dynamics at the various pump wavelengths are clearly seen. Aside from different energy cutoffs, they clarify the independence of the dynamics on the excitation energy.

In sum, we implicitly assumed that each channel i in eq 1 represents an electronic state that is subject only to time dependent population changes. This is a reasonable approximation for rigid molecules such as CPD. For floppy molecules, however, their dynamics can exhibit large amplitude motions

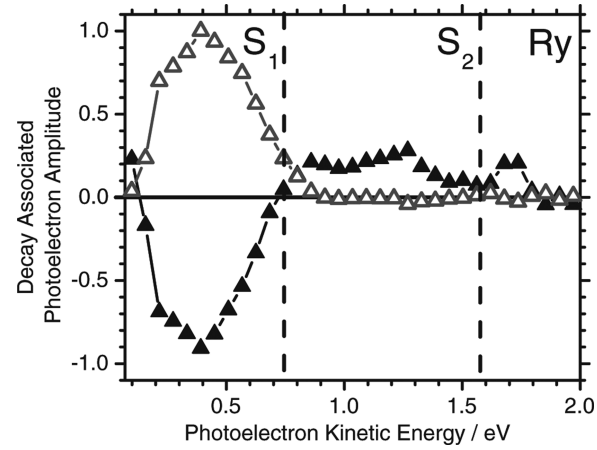

Figure 6. Decay associated photoelectron spectra $A(\tau_i)$ from biexponential fits to the TRPES data of CPD-Pr at a pump wavelength of $\lambda_p = 240$ nm. The solid symbols represent $A_{\tau_1}(E)$, and the open symbols $A_{\tau_2}(E)$, where τ_1 and τ_2 are defined by a sequential model $S_2 \rightarrow S_1 \rightarrow S_0$. The amplitudes are normalized to the maximum amplitude of A_{τ_2}. A positive amplitude indicates exponential decay; a negative amplitude exponential growth. The dashed lines separate the regions where the dynamics of the S_1, S_2, and Rydberg state can be found. See the text for a discussion.

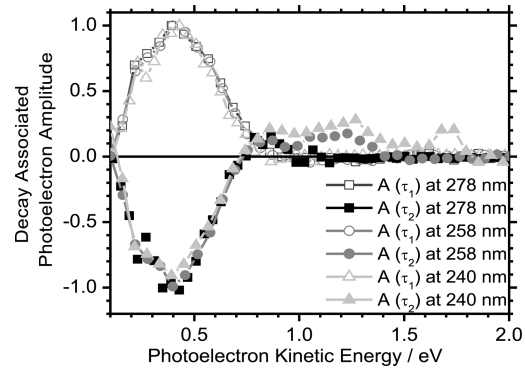

Figure 7. Decay-associated photoelectron spectra for CPD-Pr at pump wavelengths of $\lambda_p = 240$ nm (triangles), 258 nm (circles), and 278 nm (squares). For a discussion, see the text.

that change the character and the potential energy of both excited and ionic states. This leads to large shifts in the vertical ionization potential as the geometry evolves in the excited state(s). As a consequence, eq 1 will not properly describe the dynamics and the time constants and their associated spectra will not have a simple interpretation, as does the present case.

An example of such a behavior is found in the S_2 dynamics in acrolein.[11] In these cases, a full ab initio dynamical calculation of the TRPES spectra will be required.

We note that for the CPD spectra, the fwhm of the cross correlation was reduced by a factor of $3^{1/2}/2$ for the high kinetic energy region, assuming a Gaussian two-photon probe process. Here, $\tau_1 = 40$ fs and $\tau_2 = 50$ fs, in good agreement with the measurements of Fuss et al.[15] Importantly, both time constants are considerably shorter in CPD than in the methylated species, indicating a direct influence of the substituents.

4. Discussion

In cyclopentadienes, the two most important experimental observations are (i) the independence of the S_2 state decay constant upon substitution at the 5-position and (ii) the increase in S_1 state decay constants with increasing mass of this substituent. These characteristics and their consequences for the effect of substituents on dynamics at conical intersections are discussed in the following. Finally, a more complete picture of cyclopentadiene excited state dynamics is proposed.

4.1. $1B_2$ State. A pump photon of $\lambda_p = 240$ nm predominantly excites CPD to its S_2 state whereupon it rapidly dephases via the S_1 state back to the ground state (S_0; see Figure 2). According to our measurements, the S_2-S_1 conical intersection in CPD is reached within $\tau_1 \approx 40$ fs, in accordance with spectral line width analysis[23] and ion-yield measurements.[15] This short time constant hints at a conical intersection that is reached within one or two vibrational periods (40 fs $\triangleq$ 830 cm^{-1}) and further indicates the absence of any barrier on the potential energy surface separating the Franck−Condon region from the S_2-S_1 conical intersection. This is supported by the independence of the time constants from the pump laser wavelength. If a barrier were present, the dynamics should be faster upon excitation with a more energetic photon. The nonadiabatic coupling vector $\vec{h}$ and the gradient difference vector $\vec{g}$ are used to help characterize the topologies of conical intersections.[28] As they are linear terms, they are associated with directions, not frequencies, in the immediate neighborhood of the CI. Nevertheless, in a second-order expansion about the CI, the quadratic terms can be associated with frequencies (effective masses) of motions that lead to $\vec{g}$ and $\vec{h}$ at the CI. It is in this sense that, in the following, we discuss the "frequencies" of $\vec{g}$ and $\vec{h}$. The coupling mode $\vec{h}_{S_2-S_1}$ between the S_2 and S_1 state has b_2 symmetry, since $\Gamma_{S_2} \otimes \Gamma_{\mathbf{h}_{S_2-S_1}} \otimes \Gamma_{S_1} \subseteq A_1$. In contrast, the gradient difference vector $\vec{g}_{S_2-S_1}$ likely has the totally symmetric a_1 symmetry as found, for example, in the structurally similar pyrazolide.[29] Hence, the relevant $\vec{g}$-associated vibrational modes bringing the molecule toward the conical intersection should have the same symmetry. Both $\vec{h}_{S_2-S_1}$ and $\vec{g}_{S_2-S_1}$ relate to vibrations within the plane of the five C atoms. Substituents that lie within this plane, i.e., at positions one to four, should affect these vibrations, whereas substituents at the 5-position, which are displaced above the C_5 skeleton, should have little effect. This picture agrees well with our experimental results, where S_2 state dynamics slow down from 40 to 70 fs upon complete methylation in positions one to four but remain independent of substitution at the 5-position. This, in turn, is an indication that specific vibrational dynamics are more important than is the overall density of states.

4.2. $2A_1$ State. Upon crossing the S_2-S_1 conical intersection, the system dephases on the S_1 potential surface toward the intersection with the ground state. To achieve this, the molecule must bend significantly, as indicated by the imaginary frequencies seen in the calculated vibrational spectrum of the $2A_1$ state in C_{2v} symmetry.[30] Such an out-of-plane motion has also been predicted for *cis*-butadiene[1,31,32] and is typical of many polyenes.[33] The dynamical evolution of cyclopentadiene and *cis*-butadiene can occur either along a CH-out-of-plane mode of b_1-symmetry, leading to C_s-symmetry (disrotatory movement), or along a CH-out-of-plane or a ring torsion mode of a_2-symmetry along a C_2-symmetry (conrotatory) motion. For *cis*-butadiene, the disrotatory path is favored due to a smaller energy barrier in the $2A_1$ state,[1] in agreement with the Woodward−Hoffmann rules. Here, the dihedral angle at the conical intersection was calculated to be 40°.[1] The question as to whether cyclopentadiene undergoes a similar motion or whether it finds another pathway to the ground state, such as the [1, 3]-H-shift proposed by Fuss et al.,[15] cannot be discerned from our present data. This does not, however, alter the following discussion on the extracted time constants.[34]

When the lifetimes of excited states of similar molecules are compared, the vibrational density of states ρ_i is traditionally thought to play a decisive role. This derives from the weakly

TABLE 2: Four Lowest B3LYP/aug-cc-pVDZ Excitation Energies for CPD, CPD-Me4, CPD-Me5, and CPD-Pr and the Four Lowest EOM-CCSD(T)/aug-cc-pVDZ Excitation Energies for CPD[a]

energy, eV	CPD C_{2v}	CPD-Me4 C_{2v}	CPD-Me5 C_s	CPD-Pr C_s
$\Delta E_{B_2/B_u}$ TDDFT[b]	4.951	4.479	4.422[c]	4.444
oscillator strength	0.081	0.104	0.030	0.052
$\Delta E_{A_2/A_u}$ TDDFT	5.087	4.075	4.060	4.141
oscillator strength	0.000	0.000	0.014	0.011
$\Delta E_{2A_2/2A_u}$ TDDFT	5.665	4.565	4.808	4.590
oscillator strength	0.032	0.006	0.049	0.014
$\Delta E_{B_1/B_g}$ TDDFT	5.642	4.391	4.619	4.571
oscillator strength	0.000	0.000	0.000	0.003
$\Delta E_{B_2/B_u}$ CCSD(T)[d]	5.381 (307)			
$\Delta E_{A_1/A_g}$ CCSD(T)	6.355 (241)			
$\Delta E_{A_2/A_u}$ CCSD(T)	5.462 (418)			
$\Delta E_{B_1/B_g}$ CCSD(T)	6.100 (052)			

[a] The ground state geometries were calculated using B3LYP/aug-cc-pVDZ. [b] TDDFT cannot describe states with doubly excited character correctly. [c] CPD-Me5 and CPD-Pr have C_s symmetry. The A_1 and B_1 states become A′ states, the A_2 and B_2 states become A″ states. As a consequence, the *s*-Rydberg state (A_2) mixes with the S_2 state and develops significant oscillator strength (see text). [d] Values in brackets are MP2 calculations based on the MP2 geometries given in Table 3.

TABLE 3: Ground State Structures of CPD, CPD-Me4, CPD-Me5, and CPD-Pr As Calculated with B3LYP/aug-cc-pDZV and MP2/6-311+ G*[a]

		r_a, pm	r_b, pm	r_c, pm	α	β	γ	δH	δR
CPD	DFT	150.7	135.4	147.1	103.2	109.2	109.2	120.6	
	MP2	150.2	135.6	146.7	103.4	109.1	109.2	120.4	
CPD-Me4	DFT	150.6	135.9	148.5	104.2	108.7	109.2	120.9	
	MP2	150.1	136.3	147.6	104.4	108.6	109.2	120.6	
CPD-Me5	DFT	151.9	135.6	148.8	103.4	109.0	109.3	115.1	124.3
	MP2	151.0	136.0	147.3	103.8	109.3	108.8	115.7	123.0
CPD-Pr	DFT	151.8	135.6	148.9	103.5	109.0	109.2	117.2	122.5
	MP2	150.9	136.1	148.0	103.9	109.2	108.8	116.5	122.8

[a] Distances and angles are defined in Figure 8. δH is the out-of-plane angle of the H-atom, δR the out-of-plane angle of the methyl (CPD-Me5) or the propyl (CPD-Pr) group.

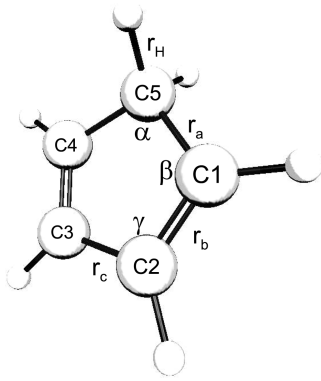

Figure 8. Parameters defining the ground state structure of cyclopentadiene. The bond distances r_a, r_b, and r_c and angles α, β, and γ are given in Table 3.

coupled perturbative limit wherein the time scale of radiationless transitions is proportional to the density of states of the ground state at internal conversion energy E_i (e.g., the Bixon−Jortner model[35]). This predicts a decrease in excited state lifetime upon methyl substitution. The present experiments, however, show the opposite effect. The time constant for the dynamics on the S_1 state (τ_2) more than doubles when one hydrogen atom in the 5-position of CPD-Me4 is substituted by a propyl group. In such strongly coupled, fast time scale dynamics, the perturbation picture does not apply and the overall density of vibrational states is not relevant. It is specific vibrational motions that will govern the nonadiabatic dynamics. Moreover, the independence of the dynamics from the excitation wavelength shows that the excess energy barely influences dynamical aspects. We suggest that the measured time constant variation with substitution may be explained by a simple notion: since the out-of-plane motion of the C5 atom plays an important role in reaching the conical intersection, a heavier substituent should inertially slow this vibration and the lifetime should concomitantly increase, as observed here.

4.3. Dynamics of Cyclopentadiene and Its Derivatives. Upon excitation at $\lambda_p = 240$ nm, two bands are visible in the TRPES spectra at time zero for the methylated cyclopentadienes (Figure 4); one exhibits a sharp maximum at the energy cutoff of 1.7 eV while the other is broad, peaking at about 1.2 eV. When CPD is compared with its substituted derivatives, using DFT calculations (see Tables 2 and 3), we observe a decrease in excitation energy with increasing alkylation. This can be explained by an additional orbital node along the methyl group in the C1 and C4 positions for the HOMO of the molecule. This leads to an overall destabilization of this orbital, whereas the LUMO remains relatively unchanged. This is true even for additional methyl substitutions in 5-position, explaining the almost invariant $\pi\pi^*$ excitation energy for the different 5-substituted CPD derivatives.

A major effect of substitution, however, is a significant stabilization of the Rydberg states. In the Franck−Condon region, the s state is energetically below the S_2 state, probably because the methyl groups support increased electron density outside the π-system. Upon substitution in the 5-position, the symmetry of the molecules is reduced to C_s, the A_1 and B_1 states transform into A′ states, and the A_2 and B_2 states transform into A″ states. B3LYP/aug-cc-pVDZ-calculations suggest that mixing between the former B_2 state and the former A_2 state transfers oscillator strength to the former A_2 state. Assuming the calculated values to be 0.3−0.4 eV too low, we propose that this state might account for the first shoulder around 4.45 eV in the absorption spectrum (Figure 3). In addition to the low lying states, part of the oscillator strength is also distributed to a third state, a p-Rydberg state of A″ symmetry. We speculate that this state could be responsible for the structure in the absorption spectra of the methylated derivatives at wavelengths $\lambda \leq 240$ nm. These calculations suggest that several states could be excited by a pump photon: the valence state (1^1B_2 state in C_{2v} symmetry, denoted as S_2) and, depending on the excitation wavelength, a series of low-lying Rydberg states. Since Rydberg states should have geometries similar to the ionic ground state, the Franck−Condon overlap should be very good and, therefore, the photoelectron spectrum should exhibit a limited vibrational progression (sharp peak). This, in turn, renders them prominent in a TRPES spectrum, despite their relatively small oscillator strength for excitation from the ground state. Hence, the sharp peak around 1.7 eV can be assigned to excitation of a Rydberg state. The broad band around 1.2 eV is then assigned to the S_2 state and the band between 0.2 and 0.7 eV to the S_1 state. The reduced Franck−Condon overlap of the S_2 state with the ionic ground state (D_0), leading to a longer, weaker progression, can be explained by the differing geometries between the two states. The spectra upon excitation at longer wavelengths are similar, aside from a missing feature at the energy cutoff, indicating that the Rydberg state is no longer energetically accessible. This suggests that the lowest lying Rydberg state with finite oscillator strength in the methylated cyclopentadienes is located around 240 nm.

For comparison, continuous irradiation experiments on cyclopentadiene in the liquid phase were shown to lead to the formation of bicyclo[2,1,0]pentene (BP) and tricyclo[2,1,0,0]pentane (TP).[18]

TABLE 4: Vibrational Frequencies for Cyclopentadiene (CPD) and 1,2,3,4-Tetramethylcyclopentadiene (CPD-Me4, B3LYP/aug-cc-pDZV)[a]

	frequency, cm^{-1}	
symmetry	CPD	CPD-Me4
a_1	816; 921; 1013; 1130; 1404 1443; 1552; *(3002)*; *(3183)* *(3221)*	*(265)*; *(310)*; 554; 699; 927; [1003]; 1130; 1245; 1363 *(1435)*; *(1444)*; 1449; *(1519)*; *(1528)*; 1618; *(2987)* *(3030)*; *(3057)*; *(3111)*; *(3076)*; *(3077)*; *(3111)*
a_2	519; 702; 936; 1144	*(142)*; *(282)*; *(305)*; *(345)*; 632; 968; [1028]; 1154 *(1507)*; *(3043)*
b_1	362; 676; 920; 937; *(3020)*	*(173)*; *(276)*; *(307)*; *(350)*; 474; 856; [1005]; 1063 *(1498)*; *(1502)*; *(1502)*; *(3000)*; *(3057)*; *(3043)*;
b_2	815; 972; 1111; 1282 1314; 1640; *(3179)*; *(3206)*	*(264)*; *(494)*; 562; 803; [1006]; [1087]; 1150; 1197 1353; *(1434)*; *(1437)*; *(1514)*; *(1516)*; 1690; *(3102)* *(3009)*; *(3028)*

[a] The values in round brackets are vibrational modes that are not ring-deforming or located at the H-atoms in the 5-position of the ring; the values in squared brackets denote modes that are mainly located on the methyl group but which also deform the ring.

In the long time limit, product yield ratios of 14:7:1 (CPD:BP:TP) were found. Considering the nonthermal product distribution (at the CCSD(T)/6-31G(d)-level, the ground state energies of BP and TP are 46 and 63 kcal/mol above the ground state of CPD, respectively[36]), the BP rearrangement very likely occurs via a separate channel on an excited potential energy surface. Evidence for this channel has been seen in ultrafast studies of CPD[15] and CPD-Me5.[37] In our data, we speculate that the appearance of a third time constant in some of the fits may indicate the presence of this additional channel on the S_1 surface. The fact that some of the data do not require a third time constant shows either the small contribution of the channel or the weakness of the Franck−Condon overlap of this channel with D_0.

In sum, we present in Figure 2 our proposed scheme for excited states dynamics in cyclopentadienes. A UV pump photon excites the molecule to the S_2 valence state and possibly a Rydberg state. The Rydberg state channel is minor and does not appear to interfere with our analysis of the S_2 or S_1 dynamics and, hence, no statement on the dynamics following Rydberg state excitation can be made. On the S_2 surface, the system evolves toward CI1 via in-plane motion of the C5 skeleton, its decay rate being τ_1^{-1}. On the S_1 surface, the wavepacket possibly bifurcates. The dominant component moves toward the intersection with the CPD ground state (CI2) via out-of-plane motions that largely depend on motions of the C atom at the 5-position and are governed by decay rate τ_2^{-1}. We speculate that the minor component may evolve toward CI2′ and pass through a different conformation,[37] perhaps responsible for BP formation in the liquid phase.[18] The vibrational dynamics at CI1 involve in-plane motions and are slowed down by substituents that decrease these frequencies. The vibrational dynamics at CI2 involve out-of-plane displacements of the C5 atom and substituents which add inertia to this motion slow down these dynamics.

5. Conclusion and Outlook

Using the method of chemical substitution, we studied the effects of substituents on vibrational dynamics at conical intersections, choosing cyclopentadiene as a model system. We presented ultrafast TRPES measurements of several substituted CPDs. For all of these, the excited state dynamics following UV excitation to the S_2 (1^1B_2) state were complete within 250 fs. For the methylated CPDs, substitution at the 5-position leads to slower dynamics on the S_1 (2^1A_1) surface, with CPD-Pr being slowest of all. This result is in contradiction with the simple notion that a higher vibrational density of states results in faster decay dynamics. This might be expected from the very fast decay rates observed: low-frequency modes cannot participate on fast time scales. When considering the vibrational density of states relevant to dynamics on a ∼50 fs time scale, we can exclude both the highest and lowest frequency modes. The highest frequency modes (e.g., CH-stretching modes) behave essentially adiabatically with respect to all other modes. On the other hand, the slower modes having vibrational periods longer than 100 fs (frequencies $\lesssim$ 300 cm^{-1}) might not significantly affect dynamics on this time scale. We note, however, the number of modes with frequencies in the region between 700 (≈50 fs) and 1700 cm^{-1} increases significantly upon methyl substitution, as can be seen in Table 4 for CPD and CPD-Me4. In fact, the number of modes of relevant symmetries (a_1 and b_2) nearly doubles. Hence, a potential effect resulting from an increased density of state should be prominent, were it important for the relaxation dynamics. We note that, by contrast, the lifetime of the S_2 (1^1B_2) state is unaffected by 5-substitution.

These results suggest that a dynamical picture of vibrational motions at conical intersections will be required. We anticipate that correlated developments in experiments and ab initio molecular dynamics methods[38,39] will play a key role in elucidating these dynamics, hopefully leading to "Polanyi rules" that govern the behavior of excited polyatomic molecules.

Acknowledgment. We thank Dr. Michael Schuurman for helpful discussions. A.E.B. is thankful for financial support from the Swiss NSF (project No. PBBS2-115105), and O.S. is thankful for financial support from the Humboldt Foundation.

References and Notes

(1) Celani, P.; Garavelli, M.; Ottani, S.; Bernardi, F.; Robb, M. A.; Olivucci, M. J. *J. Am. Chem. Soc.* **1995**, *117*, 11584.
(2) Ben-Nun, M.; Martinez, T. *J. Chem. Phys.* **2000**, *259*, 237.
(3) Yarkony, D. R. *J. Phys. Chem. A* **2001**, *105*, 6277.
(4) Polanyi, J. C. *Angew. Chem., Int. Ed.* **1987**, *26*, 952.
(5) Atchity, G.; Xantheas, S. S.; Ruedenberg, K. *J. Chem. Phys.* **1991**, *95*, 1862.
(6) Landau, L. *Z. Sowjetunion* **1932**, *1*, 46.
(7) Zener, C. *Proc. R. Soc.* **1932**, *A137*, 696.
(8) Lee, S.-H.; Tang, K.-C.; Chen, I.-C.; Schmitt, M.; Shaffer, J. P.; Schultz, T.; Underwood, J. G.; Zgierski, M. Z.; Stolow, A. *J. Phys. Chem. A* **2002**, *106*, 8979.
(9) Mestdagh, J. M.; Visticot, J. P.; Elhanine, M.; Soep, B. *J. Chem. Phys.* **2000**, *113*, 237.
(10) Sorgues, S.; Mestdagh, J. M.; Visticot, J. P.; Soep, B. *Phys. Rev. Lett.* **2003**, *91*, 103001.
(11) Lee, A. M. D.; Coe, J. D.; Ullrich, S.; Ho, M.-L.; Lee, S.-J.; Cheng, B.-M.; Zgierski, M. Z.; Chen, I.-C.; Martinez, T. J.; Stolow, A. *J. Phys. Chem A* **2007**, *111*, 11948.
(12) Stolow, A.; Underwood, J. G. *Adv. Chem. Phys.* **2008**, *139*, 497.
(13) Stolow, A. *Annu. Rev. Phys. Chem.* **2003**, *54*, 89.
(14) Ullrich, S.; Schultz, T.; Zgierski, M. Z.; Stolow, A. *Phys. Chem. Chem. Phys.* **2004**, *6*, 2769.
(15) Fuβ, W.; Schmid, W. E.; Trushin, S. A. *Chem. Phys.* **2005**, *316*, 225.
(16) Baumann, J. I.; Ellis, L. E.; van Tamelen, E. E. *J. Am. Chem. Soc.* **1966**, *88*, 846.
(17) van Tamelen, E. E.; Baumann, J. I.; Ellis, L. E. *J. Am. Chem. Soc.* **1971**, *93*, 6145.
(18) Andrews, G. D.; Baldwin, J. E. *J. Am. Chem. Soc.* **1977**, *99*, 4851.
(19) Hopkinss, J. B.; Powers, D. E.; Mukamel, S.; Smalley, R. E. *J. Chem. Phys.* **1980**, *72*, 5049.
(20) Baskin, J. S.; Dantus, M.; Zewail, A. H. *Chem. Phys. Lett.* **1986**, *130*, 473.
(21) Gruner, D.; Brumer, P. *J. Chem. Phys.* **1991**, *94*, 2862.
(22) Lochbrunner, S.; Larsen, J. J.; Shaffer, J. P.; Schmitt, M.; Schulz, T.; Underwood, J. G.; Stolow, A. *J. Electron Spectrosc. Relat. Phenom.* **2000**, *112*, 183.
(23) Sabljic, A.; McDiarmid, R. *J. Chem. Phys.* **1990**, *93*, 3850.
(24) Shang, Q.-Y.; Hudson, B. S. *Chem. Phys. Lett.* **1991**, *183*, 63.
(25) Werstiuk, N.; Ma, J.; Macaulay, J. B.; Fallis, A. G. *Can. J. Chem.* **1992**, *70*, 2793.
(26) Derrick, P. J.; Asbrinck, L.; Edqvist, O.; Johnson, B.-Ö.; Lindholm, E. *J. Mass. Spectrom.* **1971**, *6*, 203.
(27) Truttmann, L.; Asmis, K. R.; Bally, T. *J. Phys. Chem.* **1995**, *99*, 17844.
(28) Yarkony, D. *J. Phys. Chem. A* **1997**, *101*, 4263.
(29) Schuurman, M. S.; Yarkony, D. R. *J. Chem. Phys.* **2008**, *129*, 064304.
(30) Kovár, T.; Lischka, H. *J. Mol. Struct. (Theochem.)* **1994**, *303*, 71.
(31) Aoyagi, M.; Osamura, Y. *J. Chem. Phys.* **1989**, *111*, 470.
(32) Olivucci, M. J.; Ragazos, I. N.; Bernardi, F.; Robb, M. A. *J. Am. Chem. Soc.* **1993**, *115*, 3710.
(33) Martinez, T. J. *Acc. Chem. Res.* **2006**, *39*, 119.
(34) In the paper by Fuss et al. the [1,3]-H-shift was suggested by an increased time constant in perdeuterio CPD. This increase, however, is perhaps not surprising since all the vibrations are a factor of 1.1−1.35 slower in the deuterated species, thus slowing down all dynamics, independent of the actual mechanism.
(35) Bixon, M.; Jortner, J. *J. Chem. Phys.* **1968**, *48*, 715.
(36) Özkan, I.; Kinal, A.; Balci, M. *J. Phys. Chem. A* **2004**, *108*, 507.
(37) Rudakov, F.; Weber, P. M. *Chem. Phys. Lett.* **2009**, *407*, 187.
(38) For example: Ben-Nun, M.; Martinez, T. J. *Adv. Chem. Phys.* **2002**, *121*, 439.
(39) Levine, B. G.; Ko, C.; Quenneville, J.; Martinez, T. J. *Mol. Phys.* **2006**, *104*, 1039.

JP911286S